

Iris recognition based on contourlet transform and dominant energy features

C. Helen Sulochana¹, S. Selvan²

¹*Department of Electronics and Communication Engineering, Noorul Islam College of Engineering
Kanya Kumari District, Tamil Nadu, India*

²*Department of Information and Technology, PSG College of Technolog,
Coimbatore, Tamil Nadu, India*

Abstract-- Iris recognition a new biometric technology has great advantages such as variability, stability and security. In this paper we propose a new feature extraction method for iris recognition based on contourlet transform. Contourlet transform captures the intrinsic geometrical structures of iris image. It decomposes the iris image into a set of directional subbands with texture details captured in different orientations at various scales. Discriminant analysis is used to determine the optimal threshold for the selection of dominant directional energy components. Only dominant directional energy components are employed as elements of the input feature vector. These input feature vectors are compared with the template feature vectors. Experimental results show that the proposed method reduce processing time and increase the classification accuracy and outperforms the wavelet based method.

Index Terms-- Biometrics, Contourlet transform, Directional filter bank, Iris recognition, Laplacian pyramid, Thresholding.

1. Introduction

The recent advances in information technology and the increasing demand for security have resulted in the rapid development of intelligent personal identification based on biometrics. The use of the iris as a biometric feature offers advantages over other biometric features. The iris is the only internal human body organ that is visible from outside thus well protected from external modifiers. Surgical modification is impossible, detection of dead or plastic eyes is possible due to its physiological response to light and it is isolated and protected from external environment.

Various iris recognition methods have been proposed for automatic personal identification and verification. Daugman first presented a prototype system[1,2] for iris recognition based on multi-scale Gabor wavelets. Wildes presented another iris recognition system[3] in which the iris pattern was decomposed into multiresolution pyramid layers using wavelet transform. Both systems of Daugman and Wildes employed carefully designed image acquisition devices to get equal high quality iris images. Tan et al. presented a shift-invariant method [4] which decomposed the iris pattern into multiple bands using a two-dimensional Gabor filter. Boles decomposed one-dimensional intensity signals computed on circles [5] in the iris and use zero-crossings of the decomposed signals for the feature representation. The number of zero-crossings can differ among iris image samples of an identical iris due to noises. This method was improved[6,7] in which it was assumed that if two samples were acquired from an identical iris the distances between corresponding pairs of zero-crossing in one sample and another were less than given threshold value. However, the spurious zero-crossing points could degrade the performance.

A well-established fact that the usual two-dimensional tensor product wavelet bases are not optimal for representing images consisting of different regions of smoothly varying grey-values separated by smooth boundaries. This issue is addressed by the directional transforms such as contourlets, which have the property of preserving edges. The contourlet transform is an efficient directional multiresolution image representation which differs from the wavelet transform. The contourlet transform uses non-separable filter banks developed in the discrete form; thus it is a true 2D transform, and overcomes

the difficulty in exploring the geometry in digital images due to the discrete nature of the image data.

The remainder of this paper is organized as follows: Section 2 deals with method of feature extraction and classifier. Section 3. deals with Experimental results and discussion. Section 4 concludes this paper.

2. Feature Extraction and Classifier

Only the significant features of the iris must be encoded so that comparisons between templates can be made. Gabor filter and wavelet are the well-known techniques in texture analysis[1],[2],[8],[9],[10]. In wavelet family, Haar wavelet [11] was applied by Jafer Ali to iris image and they extracted an 87-length binary feature vector. The major drawback of wavelets in two-dimensions is their limited ability in capturing directional information. The contourlet transform is a new extension of the wavelet transform in two dimensions using multiscale and directional filter banks. The feature representation should have information enough to classify various irises and be less sensitive to noises.

2.1 Contourlet Transform

Contourlet transform (CT) allows for different and flexible number of directions at each scale. CT is constructed by combining two distinct decomposition stages [12], a multiscale decomposition followed by directional decomposition. The grouping of wavelet coefficients suggests that one can obtain a sparse image expansion by applying a multi-scale transform followed by a local directional transform. It gathers the nearby basis functions at the same scale into linear structures. In essence, a wavelet-like transform is used for edge (points) detection, and then a local directional transform for contour segments detection. A double filter bank structure is used in CT in which the Laplacian pyramid (LP) [13] is used to capture the point discontinuities, and a directional filter bank (DFB) [14] to link point discontinuities into linear structures. The combination of this double filter bank is named pyramidal directional filter bank (PDFB) as shown in Fig.1.

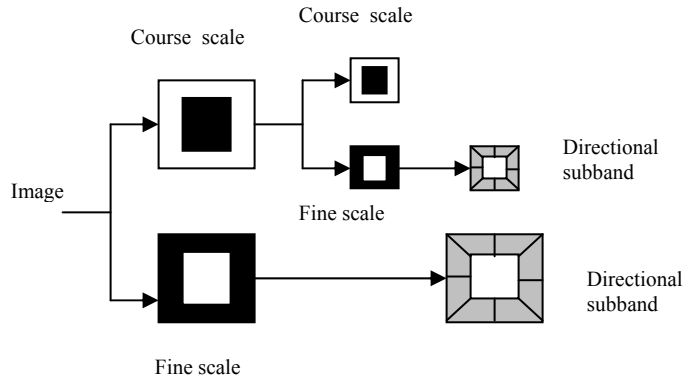


Fig.1 Two level contourlet decomposition

2.11 Laplacian Pyramid

One way of achieving a multiscale decomposition is to use a Laplacian pyramid (LP) as introduced by Burt and Adelson[13]. Fig.2 shows this decomposition process, where H and G are called (lowpass) analysis and synthesis filters, respectively, and M is the sampling matrix. LP in the PDFB uses orthogonal filters and downsampling by two is taken in each dimension. The LP decomposition at each level generates a down sampled lowpass version of the original and the difference between the original and the prediction, resulting in a bandpass image.

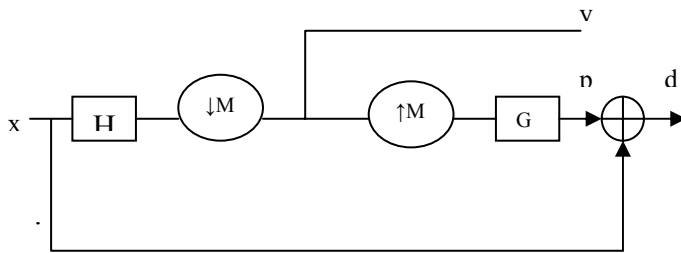


Fig.2 Laplacian pyramid

It is simple with low computational complexity due to its single filtering channel and has higher dimension. LP is a multiscale decomposition of the $L^2(R^2)$ space in to a series of increasing resolution

$$L^2(R^2) = V_{j_0} \oplus \sum_{j=j_0}^w (W_j) \quad (1)$$

where V_{j_0} is the approximation at scale 2^j and multi resolution W_j contains the added detail to the finer scale 2^{j-1} . By using L appropriate low pass filters, L low pass approximations of the image are created. The difference between each approximation and its subsequent down sampled lowpass version is a bandpass image. The result is a Laplacian pyramid with $L+1$ equal size levels; one coarse image approximation and L bandpass images.

2.12 Directional Filter Bank

The directional filter bank(DFB) is a critically sampled filter bank [12],[14],[15] that can decompose images into any power of two's number of directions. The DFB is efficiently implemented via a 1-level tree structured decomposition that leads to '21' subbands with wedge-shaped frequency partition. For the 2-D sequence $x(\mathbf{n})$, the M fold down sampled sequence $x_d(\mathbf{n})$ is defined as

$$x_d(\mathbf{n}) = x(M\mathbf{n}) \quad (2)$$

DFB is applied to the difference signal or the W_{j+1} subspaces.

$$\theta_{j,k}^l(t) = \sum_{m \in \mathbb{Z}^2} h_k^l[m - M] \phi_{j,m}(t) \quad (3)$$

The family $\theta_{j,k}^l(t)$ is an orthonormal basis of a directional subspace $V_{j,k}^{(l)}$

2.13 Powers of contourlet transform

To capture smooth contours in images, the representation should contain basis functions with variety of shapes, in particular with different aspect ratios. A major challenge in capturing geometry and directionality in images comes from the discrete nature of the data, the input is typically sampled images defined on rectangular grids. Because of pixelization, the smooth contours on sampled images are not obvious. For these reasons, unlike other transforms that were initially developed in the continuous domain and then discretized for sampled data, the new approach starts with a discrete-domain construction and then investigate its convergence to an expansion in the continuous-domain. This construction results in a flexible multi-resolution, local, and directional image expansion using contour segments. Directionality and anisotropy are the important characteristics of contourlet transform. Directionality indicates that having

basis function in many directions, only three direction in wavelet. The anisotropy property means the basis functions appear at various aspect ratios where as wavelets are separable functions and thus their aspect ratio is one. Due to this properties CT can efficiently handle 2D singularities, edges in an image. This property is utilized in this paper for extracting directional features for various pyramidal and directional filters.

LP in the CT uses orthogonal filters and downsampling by two in each dimension. The lowpass filter G in the LP uniquely define an orthogonal scaling function $\phi(t)$

$$\phi(t) = 2 \sum_{n \in \mathbb{Z}^2} g(n) \phi(2t - n) \quad (4)$$

$$\phi_{j,n} = 2^{-j} \phi\left(\frac{t - 2^j}{2^j}\right) \quad (5)$$

$\{\phi_{j,n}\}_{n \in \mathbb{Z}^2}$ is an orthonormal basis of V_j for all $j \in \mathbb{Z}$. The sequence of nested subspaces $\{V_j\}_{j \in \mathbb{Z}}$ satisfies the shift invariance and scale invariance properties. V_j is a subspace defined on a uniform grid with intervals $2^j \times 2^j$ the approximates the image at the resolution 2^{-j} . The difference image in the LP carry the details W_j to increase the resolution of an image approximation.

$$V_{j-1} = V_j \oplus W_j \quad (6)$$

2.2 Feature vector

Directional information present in the iris image can be exploited as feature vector. The original image is decomposed into eight directional subband outputs using the DFB at three different scales and the energy of each block can be obtained from the decomposed image. The energy E_{mn} of the image block associated with sub band is defined as

$$E_{mn} = \sum_{x,y \in m} |I_{mn}(x,y)| \quad (7)$$

$I_{mn}(x,y)$ denote the image coefficient at position (x,y) of image block m corresponding to subband n . Each energy value is calculated from the image block corresponding to the subband. To extract dominant directional energy, it is necessary to select a threshold. Normalized energy value is used instead of energy value to avoid threshold inaccuracies due to spatial intensity variations across the image.

Let E_{mn} denote the energy of the subband S_{mn} , where n represents the number of the subband and m represents the block of the subband. M_{mn} is the normalized energy value of E_{mn} . Coefficient value at pixel (x, y) in the image block is $I_{mn}(x, y)$. Here $m \in \{1, 2 \dots 64\}$ and $n \in \{1, 2 \dots 8\}$ at each scale. The feature vector F_{mn} is given as

$$F_{mn} = \begin{cases} F_{\max} \times M_{mn} & \text{if } M_{mn} \geq Th_{energy} \\ 0 & \text{otherwise} \end{cases} \quad (8)$$

$$M_{mn} = \frac{E_{mn}}{\sum_{n=1}^8 E_{mn}} \quad (9)$$

$$E_{mn} = \sum_{x,y \in S_{mn}} |I_{mn}(x, y) - I_{mn}| \quad (10)$$

I_{mn} is the mean of pixel values of $I_{mn}(x, y)$ in the subband S_{mn} , F_{\max} is a positive integer normalization constant. In practice we use the equation (9) for the directional energy, which is really an absolute difference measure. The normalized directional energy values with dominant intensity are scaled and quantized to an integer between $F_{\max} \times Th_{energy}$ and F_{\max} and the other values with low intensity are set to 0. The value of F_{\max} is set to 255. Since on an average only two or three directions in a block will be dominant, the memory size can be reduced by more than 50% compared with other schemes [11].

2.3 Threshold selection

Threshold selection methods can be classified into two groups, namely, global methods and local methods. A global thresholding technique thresholds the entire image with a single threshold of the image, whereas a local thresholding method partitions the given image into a number of subimages and determines a threshold for each of the subimages. Global thresholding methods are easy to implement. As such they serve as the popular tools in a variety of image processing applications. Discriminant analysis is used to select the threshold based on the maximization of the between-class variance.

Consider a discrete picture with NM pixels, with the object in one class λ_1 and the background in another λ_2 . Assume the threshold between the two classes is Th_{energy} . An estimate of energy value, i is $P_i = \sum_{x,y \in m} I_{mn}(x,y)$ | The class probabilities estimates are

defined as follows

$$p(\lambda_1) = \sum_{i=0}^{Th_{energy}-1} P_i \quad (11)$$

$$P(\lambda_2) = \sum_{i=Th_{energy}}^S P_i \quad (12)$$

The first order cumulative sample moment (up to level Th_{energy}) μ_t , and the total sample mean, μ_{tot} , are given by:

$$\mu_t = \sum_{i=0}^{Th_{energy}} iP_i \quad (13)$$

$$\mu_{tot} = \sum_{i=0}^S iP_i \quad (14)$$

The sample class means are μ_1 and μ_2

$$\mu_1 = \sum_{i=0}^{Th_{energy}-1} iP(i/\lambda_1) = \mu_t / p(\lambda_1) \quad (15)$$

$$\mu_2 = \sum_{i=Th_{energy}}^S iP(i/\lambda_2) = [\mu_{tot} - \mu_t] / [1 - p(\lambda_1)] \quad (16)$$

The between-class scatter sample variance, σ^2 is defined as

$$\sigma^2 = p(\lambda_1)(\mu_1 - \mu_{tot})^2 + p(\lambda_2)(\mu_2 - \mu_{tot})^2 \quad (17)$$

The function σ^2 is maximized to find Th_{energy}

2.4 Classifier

We determine whether two irises belong to same class by viewing the similarity of their feature vectors. Rotational alignment is achieved by generating cyclical input feature vectors and matching input feature vectors with template feature vectors. Since the proposed feature extraction process is performed on a block-by-block basis the

proposed method is robust to small angular deviations, even without rotation compensation. Two types of measures such as weighted hamming distance and Euclidian distance are used for classification.

Comparing the feature vectors X_j and Y_j , the weighted Hamming distance WHD is defined as

$$WHD = \frac{1}{N} \sum_{j=1}^N X_j (XOR) Y_j \quad (18)$$

where X_j is j th component of the sample feature vector, Y_j is j th component of template feature vector and N is the dimension of input feature vector. If the result of the XOR is zero means the j th component of sample feature vector and template feature vector are the same.

The similarity ratio SR [7] decides the matching process

$$SR = (N_j * 100) / N \quad (19)$$

Where N_j is the number of zeros results when X and Y are compared.

Euclidean distance between the template and test image is measured with the following equation.

$$D = \sqrt{\sum_{i=1}^N (X_j - Y_j)^2} \quad (20)$$

N is the dimension of the feature vector, X_j the component of the sample feature vector and Y_j is the j th component of the template feature vector.

3. Experimental Results

To evaluate the performance of this proposed system we use “CASIA” iris image database (version 1) shown in Figure 3, created by National Laboratory of pattern recognition, Institute of Automation, Chinese Academy of Science that consists of 108 subjects with 7 samples each. Images of “CASIA” iris image database are mainly from Asians. For each iris class, images are captured in two different sessions. The interval between two sessions is one month. There is no overlap between the training and test samples.

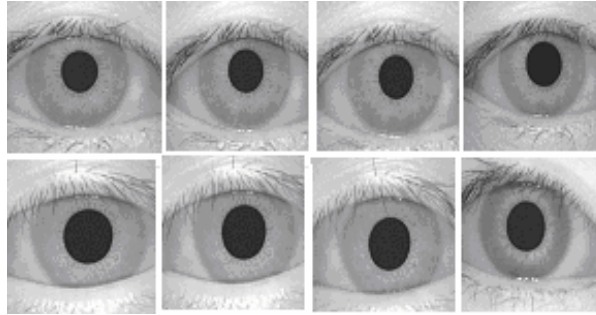


Fig.3 Iris image samples

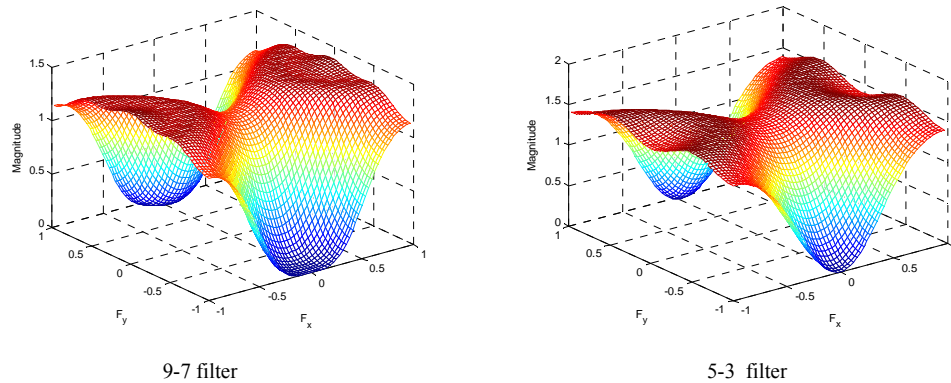


Fig.4. Frequency response of different fan filter



Fig.5 localized iris



Fig.6 Normalized iris

In our experiments, three-level contourlet decomposition is adopted. The above experiments are performed in Matlab 6.0. The normalized iris image (Fig.6) obtained from the localized iris image (Fig.5) is decomposed by the PDFB. The contourlet transform of the image is shown in Fig.7. We have used the filters designed by A. Cohen, I. Daubechies, and J.-C. Feauveau. for the quincunx filter banks in the DFB stage. Fig. 4 shows the frequency responses of fan filters of the quincunx filter bank using 9-7, 5-3, filters [16].

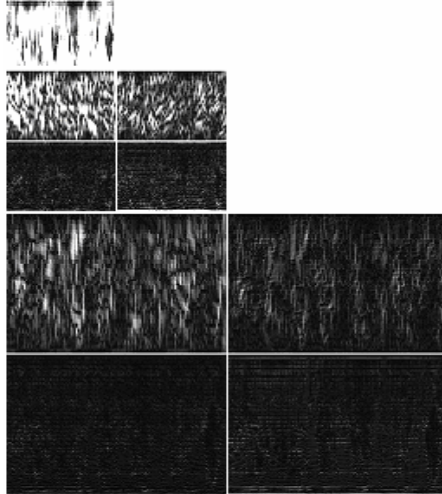


Fig.7 Contourlet coefficient

The performance of a verification method is often estimated using the false accept rate (FAR) and false reject rate (FRR). Here, FAR is the rate at which an imposter print is incorrectly accepted as genuine and FRR is the rate at which a genuine print is incorrectly rejected as an imposter. Table.1 shows the FAR and FRR for different subjects. When the number of subject is 60, the FAR and FRR are 2.32 % and 2.98%, respectively. Result shows that if more subjects are considered, error rate increases.

TABLE .1
FAR AND FRR WITH NUMBER OF SAMPLES

Number of Subjects	FAR %	FRR %
20	0.29	11.7
40	1.92	5.54
60	2.32	2.98
80	4.2	1.02
100	9.23	0.46

The performance of a verification system can also be evaluated using a receiver operator characteristic (ROC) curve, which graphically demonstrates how the False Rejection rate (FRR) changes with a variation in FAR. Receiver operating characteristics and Equal error rate EER (the acceptance threshold at which FAR is equal to FRR) are used to evaluate the performance of the system in the verification mode. Fig .8 shows the ROC between FAR and FRR. It measures the accuracy of matching process. EER is also another performance analysis parameter. Smaller the value of EER, better the algorithm. Comparing this performance of our system is high and EER is 3 .02 %.

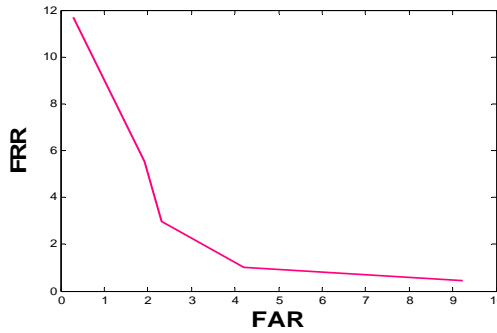


Fig.8 ROC curve

The proposed method uses only dominant directional energies. Low energy components are considered as noise. To support this point in our experiment we compare the normal image with motion blurred image and out of focus image. Table 2 shows that the Equal error rate (value obtained by adjusting the acceptance threshold such that FAR and FRR are equal) of the proposed system is almost same for different image conditions shown in Fig.9. The proposed method performs equally well regardless of the image quality.

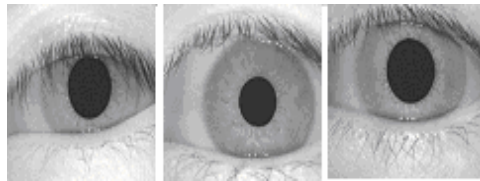


Fig.9 (a) image occluded by eyelids and eyelashes
 (b) motion blurred image
 (c) out of focus image

TABLE 2
 PERFORMANCE COMPARISON WITH DIFFERENT IMAGE CONDITIONS

Type of image	Equal error rate
With Normal	3.02
With Motion blurred	3.2
With Out of focus	3.35
image occluded by eyelids and eyelashes	3.5

Table 3 gives the result of the proposed scheme against wavelet based iris image. In this we compare the proposed system with three filter combinations of contourlet transform and the corresponding plot is shown in Fig. 10.

TABLE 3
COMPARISON OF RECOGNITION RATE FOR WAVELET AND CONTOURLET

No of subjects	Harr wavelet	P-filter: 'Harr' D-filter: '9-7'	P-filter: 'Harr' D-filter: 'pkva'	P-filter: 'Harr' D-filter: '5-3'
20	95.3	96.9	95.9	95.5
40	93	95.7	95.3	94.3
60	92	93	92	91.8
80	90	91.4	91	90.5
100	87	88.3	87.5	87.2

From the Fig. 10 we can infer that the proposed scheme outperforms the wavelet based system. The 'Haar' and '9-7' as the pyramidal and directional filter combination gives better recognition rate when compared to other pyramidal and directional filter combinations.

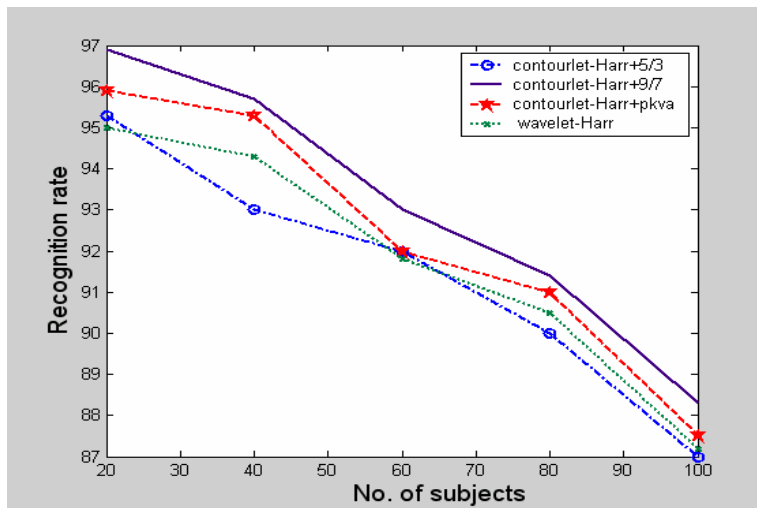


Fig.10 Comparisons of recognition rate for Wavelet and Contourlet

Table 4 and 5 gives the result of Recognition rate for different pyramidal and directional filters when applied to the iris image and the corresponding plots are shown in

Fig.11 and 12 respectively.

TABLE 4
RECOGNITION RATE FOR DIFFERENT FILTERS OF CONTOURLET TRANSFORM

No of subjects	P-filter: '9-7' D-filter: 'pkva'	P-filter: 'pkva' D-filter: '9-7'	P-filter: '5-3' D-filter: '9-7'
20	92.54	91.9	92.65
40	91.2	90.3	92.3
60	90.8	89	92.8
80	89.5	87.8	92
100	87.2	85.5	91.7

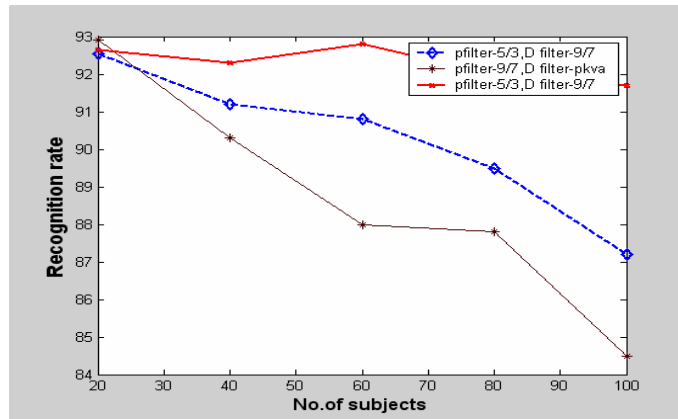


Fig.11. Comparison of recognition rate vs. No. of subjects between different pyramid and directional filters using contourlet transform

TABLE 5
RECOGNITION RATE FOR DIFFERENT FILTERS OF CONTOURLET TRANSFORM

No of subjects	P-filter: '9-7' D-filter: '5-3'	P-filter: 'pkva' D-filter: '5-3'	P-filter: '5-3' D-filter: 'pkva'
20	92.53	91.89	92.69
40	91.18	90.26	92.36
60	90.78	88.88	92.9
80	89.48	87.58	92.8
100	87.19	85.45	92

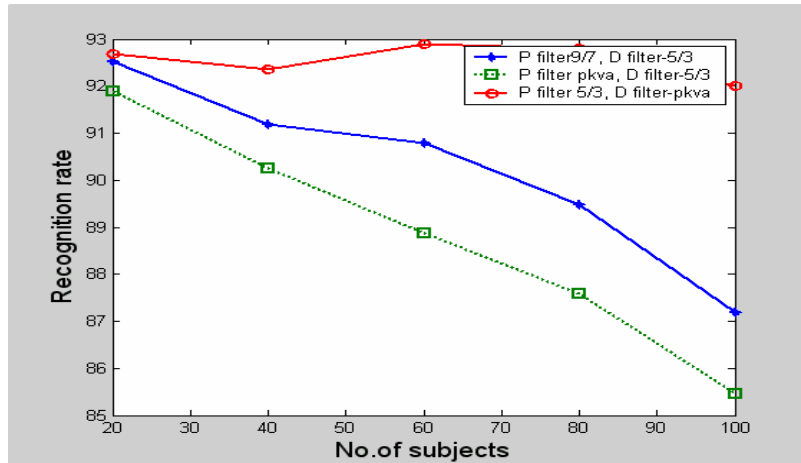


Fig 12. Comparison of recognition rate vs. No. of subjects between different pyramid and directional filters using contourlet transform

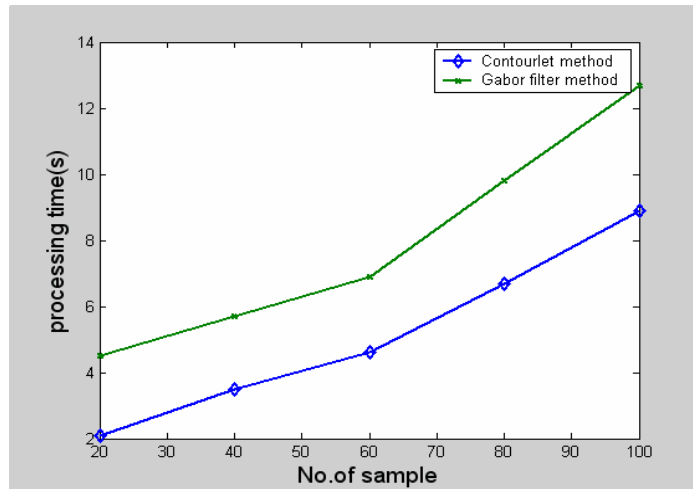


Fig .13 Comparison of processing Time with wavelet based method

Similarity measures play an important role in iris matching. We perform two types of similarity measure for texture features generated by the proposed method. Table 6 shows the recognition results of the different similarity measures. Recognition rate using hamming distance matching algorithm is slightly large compared with Euclidean distance measure. The results show that both measures have almost the same recognition rate.

TABLE 6
EFFECT OF MATCHING ALGORITHM IN SYSTEM RECOGNITION RATE : P FILTER-HARR, D FILTER-9/7

Matching Algorithm	Correct Recognition rate (%)
Hamming distance	94.5
Euclidian Distance	93.7

To compare the effectiveness of the feature extraction methods, the performances of the system is compared with wavelet based method using two measures: 1) equal error rate (EER) and 2) processing time. EER is often used as a compact measure of verification accuracy of a biometric system. Table 7 shows that the Equal error rate for the proposed method is less compared with the wavelet based method. The processing speed of the proposed method was faster than that of the wavelet based method. The comparison of processing time of these two methods is shown in Figure 13. In both the cases the processing time increases with increase in the number of subjects. Since in the proposed system low energy values are considered as noise the feature vector of each subband consists of two or three dominant energy values, which reduce the processing time as compared to other system, which we compare.

TABLE 7
PERFORMANCE COMPARISON WITH WAVELET TRANSFORM METHOD

Method	Equal error rate (%)	Processing Time (sec)
Wavelet transform method	4.1	4.48
Proposed method	3.02	2.9

4. Conclusion

A new algorithm for iris recognition using contourlet transform has been presented. Each iris image is decomposed with pyramidal directional filter bank and then a fixed length feature vector is obtained. An extensive result has been taken with different filters. Here, only four filter combinations are considered. Compared with wavelet

transform method, contourlet-based method achieves a higher accuracy because contourlet transform has capacity to capture comparatively richer directional information. Experimental results reveal that our algorithm reduces the processing time and invariant to noise. We are currently perusing with other filter combination to increase the recognition rate.

References

1. J. Daugman. "High confidence visual recognition of persons by a test of statistical independence" *IEEE Transactions on Pattern Analysis and Machine Intelligence*, Vol. 15, No. 11, pp: 1148-1160, Nov 1993.
2. J. Daugman. "How Iris Recognition works". *IEEE Transactions on Circuits and systems for video Technology*, Vol.14, No.1, pp: 21-30, January 2004.
3. R. P. Wildes, et al., "A machine-vision system for iris recognition," *Machine Vision and Applications, Springer-Verlag, 1996*.
4. Zhenan Sun, Yunhong Wang, Tieniu Tan, and Jiali Cui "Improving Iris Recognition Accuracy Via Cascaded Classifier, *IEEE Transactions on systems, Man And Cybernetics-part C: Applications and reviews*, Vol.35, No.3, Aug 2005
5. W.W. Boles and B. Boashash, "A Human Identification Technique Using Images of the Iris and Wavelet Transform", *IEEE Trans. Signal Processing*, Vol.46, No.4, 1998, pp.1185-1188
6. Sanchez-Avila, C., Sanchez-Reillo, R., de Martin-Roche, D., "Iris-based biometric recognition using dyadic wavelet transform", *IEEE Aerospace and Electronics Systems Magazine*, Volume: 17 Issue 10, pp. 3-6, Oct 2002
7. De Martin-Roche, D., Sanchez-Avila, C., Sanchez-Reillo,R., "Iris recognition for biometric identification using dyadic wavelet transform zero crossing", *IEEE Int. Carnahan Conference on SecurityTechnology*, pp. 272-277, Oct 2001
8. L. Ma, T. Tan, Y. Wang and D. Zhang, "Personal identification based on iris texture analysis," *IEEE Trans. Patt. Analy. & Mach. Intel* vol. 25, No. 12, pp. 1519-1533, Dec. 2003.

9. Y. Zhu, T. Tan, and Y. Wang, "Biometric Personal Identification Based on Iris Patterns," *Proc. Int'l Conf. Pattern Recognition*, vol. II, pp. 805-808, 2000.
10. L. Ma, Y. Wang, and T. Tan, "Iris Recognition Based on Multichannel Gabor Filtering," *Proc. Fifth Asian Conf. Computer Vision*, vol. I, pp. 279-283, 2002.
11. Jafar M. H. Ali, Aboul Ella Hussanien "An Iris Recognition System to Enhance E-security Environment Based on Wavelet Theory" *AMO - Advanced Modeling and Optimization*, Volume 5, Number 2, 2003
12. M. N. Do and M. Vetterli, "The contourlet transform: An efficient directional multiresolution image representation," *IEEE Trans. Image Proc.*, *IEEE Transactions on Image Processing*, revised Dec. 2004, to appear.
13. P. J. Burt and E. H. Adelson, "The Laplacian pyramid as a compact image code," *IEEE Trans. Commun.*, vol. 31, no. 4, pp. 532-540, April 1983.
14. R. H. Bamberger and M. J. T. Smith, "A filter bank for the directional decomposition of images: Theory and design," *IEEE Trans. Signal Proc.*, vol. 40, no. 4, pp. 882-893, April 1992
15. T. T. Nguyen and S. Orintara, "A directional decomposition: theory, design and implementation," International Symposium on Circuits and Systems, Vancouver, Canada, May 2004.
16. A. Cohen, I. Daubechies, and J.-C. Feauveau. Biorthogonal bases bases of compactly supported wavelets. *Commun. on Pure and Appl. Math.*, 45:485-560, 1992